symmetry

MDPI

*Article*

# Symmetry of Post-Translational Modifications in a Human Enzyme

**Teresa Maria Carusone and Giuseppe Manco ***

Institute of Biochemistry and Cell Biology, National Research Council of Italy, 80131 Naples, Italy; tcarusone@embl.fr

* Correspondence: giuseppe.manco@cnr.it

**Abstract:** Paraoxonase 2 (PON2) is a member of a small family of human lactonases. Recently, post-translational modifications (PTMs) of PON2 were highlighted, one of which involved the modulation of the enzyme activity. Furthermore, two important single nucleotide polymorphisms (SNPs) involved in type 2 diabetes and its consequences, were found to modulate the enzyme activity as well. The position on the PON2 structural model of both residues corresponding to SNPs and PTMs suggested a symmetry of the molecule. By sequence and structure superposition we were able to confirm this finding. The result will be discussed in light of the evolution of symmetry in biological molecules and their function.

**Keywords:** paraoxonase 2 (PON2); structure symmetry; post-translational modifications; single nucleotide polymorphisms



**Citation:** Carusone, T.M.; Manco, G. Symmetry of Post-Translational Modifications in a Human Enzyme. *Symmetry* **2022**, *14*, 212. https://doi.org/10.3390/sym14020212

Academic Editor: John H. Graham

Received: 17 December 2021
Accepted: 18 January 2022
Published: 22 January 2022



## 1. Introduction

### *1.1. Symmetry in Proteins*

Symmetry in proteins is widespread and involves not only homomeric association in quaternary structures of non-symmetric monomers, but also symmetry within monomeric proteins in about 25% of cases [1]. In general, symmetry in oligomeric complexes is a rule resulting in several advantages and there are excellent reviews on the topic to which the reader can refer to [1–5]. These reports generally emphasize the role of symmetry in stabilizing structures [5,6], orienting functions [7], reducing the effects of DNA errors [1,5], favoring complex functions [8,9], and enabling allostery [10]. The sequence identity between monomers is maintained quite high and can easily be spotted by sequence alignment algorithms. Symmetry in monomers has also been reported in many papers [11–13]. The iteration of structural modules within a longer polypeptide, thought to arise from gene duplication and fusion of shorter fragments, is considered to be at the core of protein evolution [2,3].

The evolution of (β/α)8 barrel proteins, that is currently thought to have stemmed from the fusion of two (β/α)4 half-barrels, is an example. In that case, fusion appears to confer stability to the protein structure. After the formation of a whole (β/α)8 barrel, this structure could have evolved and diverged to form fully active enzymes. Interestingly, it was shown that isolated (β/α)4 half-barrels derived from the N- and C-terminal domains of the β-glucosidase Sfβgly (residues 1 to 265 and residues 266 to 509) undergo an activation process, which renders them catalytically active. The activation processes were simultaneous with modifications in the initial structures, coincident with an increase in the sizes of Sfβgly-N and Sfβgly-C particles, and paralleled by reduced exposure of their tryptophan residues. These observations suggest that the acquisition of a catalytic activity associated with the transition from a half to a whole (β/α)8 barrel might have driven such an evolutionary process [14].

Studies aiming at fragmenting symmetric "β-propeller" proteins to pick out an ancient folding motif provided proof that polypeptides of roughly 100 amino acids, comprising two

copies of a repeated motif, assembled in a multimeric form, but not single-motif segments of 50 amino acids [15–17].

In general, propellers with a medium number of blades exploit the evolution of differential loops to achieve protein–protein interactions and to catch substrates at the top face or between domains [18]. Moreover, the existence of α-helices in a propeller structure could contribute to the display of specific functions. This is the case for the two protruding α-helices of the six-bladed propeller domain of serum paraoxonase PON1, conserved also in PON2 (see below), which are proposed to form the hydrophobic patch that drives particles/membrane anchoring [19].

### *1.2. Symmetry and Post-Translational Modifications (PTM)*

PTMs of enzymes and proteins are emerging as major modulators of protein function and related cellular processes. The disclosure and examination of PTMs such as acetylation, propionylation, methylation, phosphorylation, sumoylation, ubiquitination, and many others have established both nuclear and non-nuclear roles for PTMs. In recent years, there has been an overwhelming appreciation for the wide diversity of modifications, but most importantly, the interplay between them [20–24]. This crosstalk is compelling for the right fulfillment of such diverse cell functions such as gene expression, genome organization, cell division, and DNA damage response. PTMs can directly impact cell function by modifying histones, enzymes, and their associated activities, by guiding the gathering of protein complexes as well as recognition and targeting to the genome or to other cellular compartments. The cell has evolved a number of enzymes that are important for the assembly and maintenance of these PTMs and are often referred to as "writers" (e.g., histone methyltransferases, acetyltransferases, etc.) or "erasers" (e.g., histone demethylases, deacetylases, etc.) [25,26].

### *1.3. Breaking the Symmetry of PTMs*

In the field of PTMs, two seemingly distinct themes—symmetry and multisite modifications—show a growing relatedness. Multisite modifications occur when a protein has two or more modifications in different regions that can be added randomly or sequentially. The combination of all the PTMs that decorate a protein acts like a barcode that gives the protein a specific function. The symmetry of the modification network, regardless of how it comes about, can be broken, resulting in altered biochemistry of signaling/function. This has been demonstrated in some cases by computational modeling and confirmed analytically [27].

Symmetry breaking as a basis for the generation of cellular-level structures, such as polarization and polarized or other strongly different species concentration patterns, has been explored in a variety of contexts. Examples include the generation of polarity in fungi and plant cells [28] and in neutrophil chemotaxis [29]. Symmetry has also been invoked as a key component in the development of the Monod–Wyman–Changeux model, which has been used to explain allostery in biomolecular information processing [10].

While the subject of symmetry in chemistry is well known, especially at the level of molecular structures [30], there are relatively few studies of symmetry breaking at the level of molecular reactions. In chemical reaction systems, one encounters symmetry in the context of chirality in racemic mixtures. Even if the network/reaction system is symmetric and allows equal amounts of the two forms, this symmetry can break and give rise to a dominant form. Recent studies [31,32] have investigated and demonstrated the occurrence of such symmetry breaking in a number of potential reaction systems. Chiral symmetry breaking has been observed experimentally in the crystallization of nanoparticles [33], in fibril formation from racemic mixtures [34], and in the alkylation of pyrimidine-5-carbaldehyde with diisopropylzinc [35]. Such symmetry breaking is of particular importance in prebiotic evolution and biology, where biopolymers and biomolecules are characterized by specific chirality and orientation, even though the original chemical world of non-life was chirally symmetric [36]. It is believed that the emergence of such chirality is important for un-

derstanding the origin of life [37]. Symmetry breaking can: (a) confer new capabilities to protein networks, (b) be the basis for ordering multisite modifications, which is widely observed in cells; (c) impact information processing in multisite modifications and in cell signaling networks/pathways, where multisite modifications are present; and (d) can be a fruitful new approach for engineering in synthetic biology and chemistry [27].

Here, we would like to briefly discuss symmetry and enzyme function, and more specifically, how the function of the human lactonase PON2 is modulated by a post-translational modification (PTM) that can disrupt symmetry.

### *1.4. The Human Paraoxonase PON2*

PON1, PON2, and PON3 are three highly conserved lactonases that form the human paraoxonase family (PON) [38,39]. PON2 is a protein found in almost all tissues, whereas PON1 and PON3 are predominantly secreted from the liver into the bloodstream. In particular, PON2 has been found in the endoplasmic reticulum, mitochondria, and outside the plasma membrane [40–42]. PON2 is the oldest member of the family and shows the highest lactonase activity [43,44]. Due to its positioning on the plasma membrane and high lactonase activity, PON2 is considered a primary line of defense against Gram-negative bacterial infections. The bacterial signal 3-oxo-dodecanoyl homoserine lactone (3OxoC12HSL) is the major player of quorum sensing (QS) in Gram-negative bacteria [43]. It is also capable of invading eukaryotic cells, triggering apoptosis in many cell types (including cancer cells) [44] and modulating host immune responses, hence the name quorhormone [45].

Through its lactonase activity, PON2 controls the bacterial QS process, modulating biofilm formation and virulence factors production [46]. However, several in vitro and in vivo studies suggest that PON2 has anti-ROS activity in addition to the lactonase activity. For more information, see a recent review on PON2 [47].

In eukaryotic cells, 3OxoC12HSL can rapidly inactivate PON2 lactonase activity in the absence of protein reduction [48]. Recently, we discovered that it is possible to reconstitute and study 3OxoC12HSL-mediated PON2 inactivation in a cell-free system from recombinant PON2 incubated with a HeLa crude extract. The inactivation was accompanied by ubiquitination at position K144, which was detected by mass spectrometry [49].

## 2. Materials and Methods

The AlphaFold database output of the AlphaFold deep learning algorithm [50] was used to download the PON2 model (https://alphafold.ebi.ac.uk/entry/Q15165 accessed on 11 November 2021) that was used for most of the analyses reported here.

The Swiss PDB viewer program [51] was used to make calculations, compare and analyze models, and analyze the internal symmetry of PON2. With this program was generated the structural alignment after superposition of the two halves of PON2.

The FoldX algorithm [52] used to evaluate mutants' stability ([53]; Table 1) was an add-on under the Yasara visualization and analysis program [54]. It was used mostly to correct models, generate mutants, and theoretically measure protein stability.

PyMol (The PyMOL Molecular Graphics System, Version 2.0, Schrödinger, LLC.,New York, NY, USA) was used for drawing some of the pictures. Additional workart was made with Paint under Windows 8.

## 3. Results and Discussion

No 3D X-ray structure is so far available for PON2 due to the instability of the protein in solution and the formation of crystals too small to be useful for X-ray analyses [unpublished]. In a previous work, we managed to obtain a small-angle X-ray scattering (SAXS) structure that fitted quite well the model obtained by using as reference the PON1 structure [19] (Figure S1). The protein appears to be monomeric, at least in the active form. In fact, dimers and trimers were also detected in gel filtration analyses but were

mostly inactive [48]. Unfortunately, the resolution of SAXS was too low (30 Å) to be more informative.

Recently, the models of all proteins in the human proteome were automatically generated using AlphaFold, a novel machine learning approach that incorporates physical and biological knowledge about protein structure, leveraging multi-sequence alignments, into the design of the deep learning algorithm [50,55]. The PON2 3D model was downloaded from the AlphaFold database (https://alphafold.ebi.ac.uk/entry/Q15165 accessed on 11 November 2021). AlphaFold information for PON2 also includes a predicted model-quality score for individual residues. This metric predicts the regions of the sequence where the model is likely to be of high quality and the regions where the model is probably less reliable, and it produces a per-residue confidence score (pLDDT) between 0 and 100. PON2 model confidence in AlphaFold is mostly very high (pLDDT > 90) with only some residues (G2-V5, P72, G73, F136) having a pLDDT between 70–90. The high confidence of the model can be explained by the 66% sequence identity and 81% similarity of PON2 with the homolog PON1, whose structure is publicly available (PDB ID: 1V04).

The PON2 model was identified in this database and downloaded. It turned out to be quite similar to the models we had already published [48,49]. The model is shown in Figure 1.


**Figure 1.** Model of PON2 from Alphafold. Ribbon representation with highlighted the two ubiqitination sites K144 and K311. The picture was drawn with the Pymol program.

We used this model for the analysis reported here. The analysis allowed us to observe a symmetrical structure, which is the fundamental feature of the six-sheet β-propeller structure family of proteins, as described above.

Using mass spectrometry analysis of the PON2 protein expressed in *E. coli* and purified after incubation in a HeLa crude extract treated or not with 3OxoC12HSL, we identified residue K144 as the unique ubiquitinated site [48]. We demonstrated that this ubiquitination depends on the presence of 3OxoC12HSL, a quor-hormone produced by Gram-negative bacteria that controls the production of many virulence factors and, in particular, the formation of the bacterial biofilm, as mentioned previously [48].

Other ubiquitination sites in PON2 have been identified by us and by others. Of particular interest is the identification of K313 as a ubiquitination target [48,56]. These two ubiquitination sites are particularly interesting considering that both the K313 and K144 targets are close to the two variants (A148G and S311C) corresponding to the SNPs described for PON2 (Figure 2). In 1996, two polymorphisms were discovered in the coding sequences of PON2 predicting an A148/G148 and an S311/C311 substitution in the protein derived from transcript I [57]. Given the potential importance of conserved cysteines in

PON1 [58], it was reasonable to speculate that the introduction of an additional cysteine by the polymorphism at codon 311 could affect the structure and/or function of PON2. However, looking at the 3D model of PON2, the Cys311 residue seems to be far away from the other cysteines (e.g., Cys284), ruling out any interfering effect or formation of a new bond.

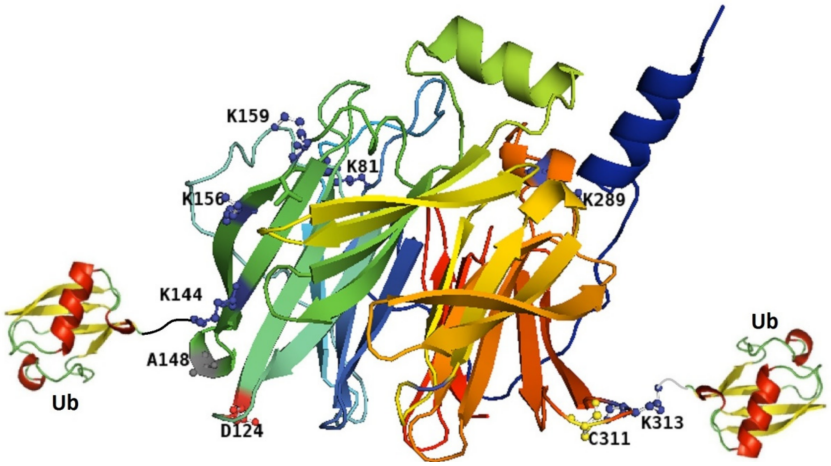


**Figure 2.** Cartoon of the PON2 model which highlighted the ubiquitination and the ADP ribosylation (D124) sites so far identified (shown in ball and stick representation). The two Ubiquitin moieties (PDB:1UBQ) are appended to the structure only for a demonstrative purpose. The figure was generated with the YASARA program available free of charge at www.YASARA.org. The variants ALA148 and CYS311 are also highlighted.

Given the opportunity to express mutant versions of PON2 in *E. coli*, we previously generated mutants and analyzed the activities. We showed that both mutations affected the lactonase activity of PON2 [49]. In particular, the specificity decreased dramatically by 16- and 5-fold for the 148G and 311C variants, respectively. Since the two SNPs appear to be in linkage disequilibrium, it is expected that they have a stronger effect in homozygosis.

By looking at the symmetrical PON2 structure and the positioning of the couples 144/148 and 311/313, we suspected that the symmetry concerned also the two variants and the two nearby ubiquitination sites. In order to further analyze this point, we first analyzed the two halves of the PON2 protein sequence. By roughly dividing in half the primary sequence and manually superposing region 1–160 and region 161–354, we highlighted many conserved residues. By using a manual procedure of trials and errors and by inserting a minimum number of gaps, we were able to generate the alignment shown in Figure 3A.

Looking at the position of the above pairs, they appear quite far apart (more than twenty amino acids), which is not in agreement with the original hypothesis. To clarify this point, we applied the same approach to the 3D model. We split the structure in half, saved the pdb files, and then overlaid the structures to look for similarities (Figure 4). A total of 268 alpha-carbons were overlaid with an RMS value of 1.43 Å.

The corresponding sequence alignment is shown in Figure 3B. The two alignments by sequence (Figure 3A) and by structure (Figure 3B) matched quite well in the middle part, with some differences at the edges. In the region 1–160, two insertions of twelve amino acids were allowed, while in the other region an insertion of fourteen residues was observed. However, it is noteworthy that there is an overlap between the two variants corresponding to the SNPs flanked by the ubiquitination sites.

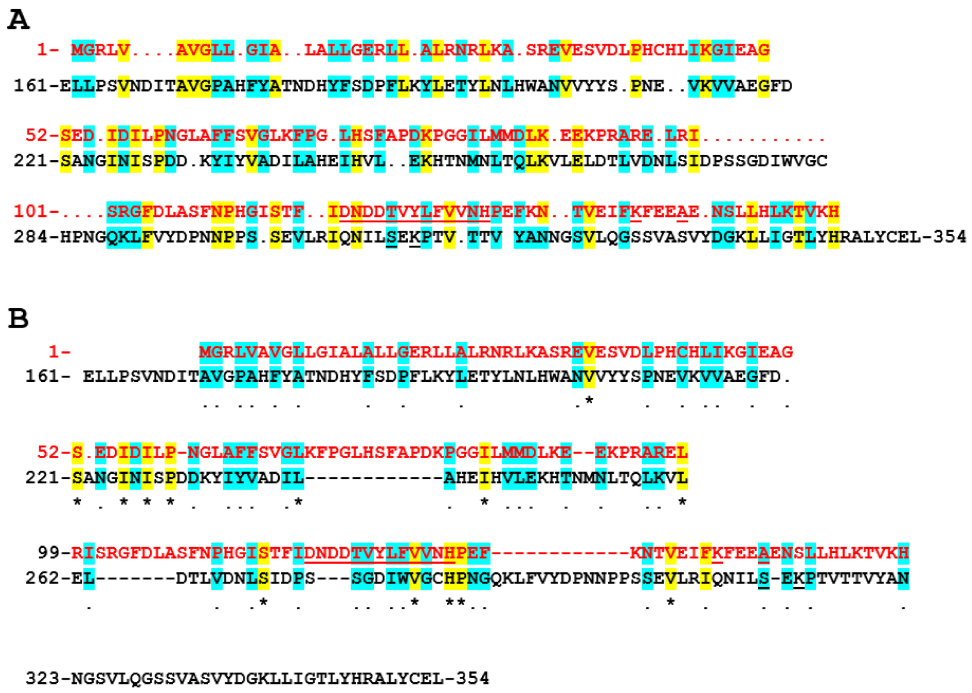


**Figure 3.** (**A**) Sequence alignment of PON2 suggesting the existence of an internal duplication. The residues in the region from 1 to 160 are shown in red. The residues in the region from 161 to 354 are shown in black. The twelve residues that are deleted in PON2 isoform 2 [56] are underlined. Yellow underlining indicates identity, while cyan indicates similarity. The Ala148 and Ser311 polymorphisms are underlined. The two ubiquitination sites are shown in bold and underlined. (**B**) Confirmation of an internal duplication by structural alignment. The Swiss-Pdb viewer program was used to overlay the two halves of the PON2 model.

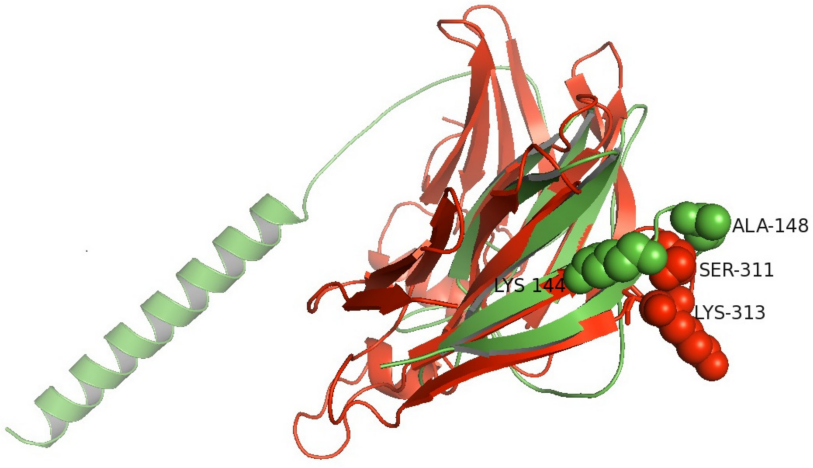


**Figure 4.** Suggestion for an internal duplication in the PON2 structure. The two parts of the PON2 model spanning regions 1–160 (green) and 161–354 (red) were superimposed using the program SWISS-PDB viewer. The two lysines 144 and 313 and the two SNPs 148A and 311S are highlighted in the ball representation.

A possible explanation for this result is that the original PON2 gene duplicated during evolution, closing a structure that initially appeared as a dimer of two semicircles. This also allowed the variant and the nearby modification site, which however could have been added later, to modulate PON2 activity. If this is the case, the idea of "breaking symmetry" by PTM dynamics could apply even more here because of the linkage disequilibrium of the two SNPs. However, proving the existence of this effect will require further studies.

*In Silico Prediction of PON2 Variants Stability*

In order to highlight the effect of the two SNPs on the PON2 structure, we performed an in silico prediction of PON2 variants stability.

Site-directed mutagenesis for PON2 variants generation (PON2_A148G and PON2_S311C) was performed by the FoldX algorithm [54] used as a plugin in the protein structure visualizer YASARA [56]. The force field algorithm became popular as a web tool in 2005 by Schymkowitz et al. (2005) and was refined to the current last version FoldX 5.0 used for this analysis.

The PON2_wildtype PDB model downloaded from AlphaFold was opened in YASARA and repaired by FoldX to reduce the energy content of the protein-structure model to a minimum by rearranging sidechains (PON2_wt > PON2_wt_repaired). By using this repaired model, three mutants were generated by single aminoacidic substitutions: PON2_A148G, PON2_S311C, and the double mutant PON2_A148G _S311C.

We used the FoldX empirical method to estimate the stability effect of the generated mutations. The stability (ΔG) of a protein is defined by the free energy, which is expressed in kcal/mol. The lower it is, the more stable the protein is. ΔΔG is the difference in free energy (in kcal/mol) between a wild-type and a mutant (ΔΔG = ΔGwildtype – ΔGmutant). A mutation that brings energy (ΔΔG > 0 kcal/mol) will destabilize the structure, while a mutation that removes energy (ΔΔG < 0 kcal/mol) will stabilize the structure. The reported accuracy of FoldX is 0.46 kcal/mol (i.e., the SD of the difference between ΔΔGs calculated by FoldX and the experimental values) [55]; therefore, the ΔΔG values can be categorized into seven categories (Table 1). Commonly it is assumed that a mutation has a significant effect if ΔΔG is >1 kcal/mol, which roughly corresponds to the energy of a single hydrogen bond.

**Table 1.** ΔΔG values for mutation effects on protein stability (from ref. [53]).

| | |
|---|---|
| Highly stabilising | $\Delta\Delta G < -1.84$ kcal/mol |
| Stabilising | $-1.84$ kcal/Mol $\leq \Delta\Delta G < -0.92$ kcal/mol |
| Slightly stabilising | $-0.92$ kcal/Mol $\leq \Delta\Delta G < -0.46$ kcal/mol |
| Neutral | $-0.46$ kcal/Mol $< \Delta\Delta G \leq +0.46$ kcal/mol |
| Slightly destabilising | $+0.46$ kcal/mol $< \Delta\Delta G \leq +0.92$ kcal/mol |
| Destabilising | $+0.92$ kcal/Mol $< \Delta\Delta G \leq +1.84$ kcal/mol |
| Highly destabilising | $\Delta\Delta G > +1.84$ kcal/mol |

The ΔG was calculated for PON2 wildtype, PON2_A148G, and PON2_S311C (Table 2) based on the following equation:

$$\Delta G = \Delta G\ vdw + \Delta GsolvH + \Delta GsolvP + \Delta Gwb + \Delta Ghbond + \Delta Ggel + \Delta Gkon + T\Delta Smc + T\Delta Ssc + T\Delta Str$$

The differences in the total energy between the PON2 wildtype and the two single and double mutants were calculated (Table 3).

The two single mutants and the double mutant show a ΔΔG > 0. Taking into consideration the reported accuracy of FoldX of 0.46 kcal/mol the overall effect of the A148G mutation (+0.31 kcal/mol) on the PON2 structure can be considered neutral, while the mutation S311C (+0.57 kcal/mol) and the double mutation A148G_S311C (+0.88 kcal/mol) have a slightly destabilizing effect on the PON2 structure (Table 3).

This result seems to suggest a slight effect of mutations on the PON2 structure that should be responsible for the dramatic reduction in lactonase activity. Understanding at the molecular level this effect will require a high-resolution structure of PON2 with metals, and hopefully the substrate, in the active site. The destabilization could be responsible in the cell for faster degradation and reduced activity. The effect is stronger in the double mutant. However, by superposing the wildtype and mutant structures, no particular clues emerged suggesting that the effect was a slight conformational change affecting the active

site dynamics. In Figure S2, the superposition of PON2 wildtype and double mutant A148G_ S311C is shown.

**Table 2.** Energy calculations by FoldX.

| | **PON2_wt** | **PON2_A148G** | **PON2_S311C** | **PON2_A148G_S311C** |
|---|---|---|---|---|
| BackHbond | −260.37 | −260.37 | −259.80 | −259.80 |
| SideHbond | −112.67 | −112.67 | −112.06 | −112.06 |
| Energy Van der Waals | −425.17 | −425.00 | −424.95 | −424.78 |
| Electrostatics | −9.30 | −9.32 | −9.30 | −9.32 |
| Energy solvation polar | 558.54 | 558.30 | 557.63 | 557.39 |
| Energy solvation hydrophobic | −568.97 | −568.75 | −569.18 | −568.96 |
| Energy Van der Waals clash | 13.90 | 13.90 | 13.89 | 13.89 |
| Energy torsion | 7.12 | 7.12 | 7.12 | 7.12 |
| Backbone Van der Waals clash | 128.85 | 128.74 | 128.75 | 128.64 |
| Entropy side chain | 212.57 | 212.55 | 212.42 | 212.40 |
| Entropy main chain | 532.09 | 532.27 | 532.53 | 532.71 |
| Water bonds | 0.00 | 0.00 | 0.00 | 0.00 |
| Helix dipole | −3.31 | −3.31 | −3.31 | −3.31 |
| Loop entropy | 0.00 | 0.00 | 0.00 | 0.00 |
| Cis bond | 0.00 | 0.00 | 0.00 | 0.00 |
| Disulfide | −5.71 | −5.71 | −5.71 | −5.71 |
| Electrostatic Kon | 0.00 | 0.00 | 0.00 | 0.00 |
| Partial covalent interactions | 0.00 | 0.00 | 0.00 | 0.00 |
| Energy ionisation | 3.11 | 3.11 | 3.11 | 3.11 |
| Entropy complex | 0.00 | 0.00 | 0.00 | 0.00 |
| **Total Energy (ΔG)** | **−58.20** | **−57.89** | **−57.63** | **−57.32** |

**Table 3.** Total energy differences between PON2 wildtype and its mutants.

| **ΔG (kcal/mol)** | **PON2 Wildtype** | **PON2_A148G** | **PON2_S311C** | **PON2_A148G_S311C** |
|---|---|---|---|---|
| | **−58.20** | **−57.89** | **−57.63** | **−57.32** |
| **ΔΔG** $(\Delta G^{m} - \Delta G^{wt})$ | | +0.31 | +0.57 | +0.88 |

## 4. Conclusions

Symmetry breaking is emerging as a leading mechanism to integrate signals and achieve different outcomes, depending on the cellular environment. Some proteins represent a fulcrum in which PTMs accumulate in a combinatorial manner and show effects only when symmetry is broken. We have described here the case of PON2, a human lactonase with different activities (lactonase, anti-ROS, protein–protein interactions) and different localizations implying important functions. Two quasi-symmetric SNPs have been reported to modulate the protein lactonase activity. Near these variants, quasi-symmetric PTMs have been described to modulate this activity. Notably, ubiquitination at position 144 was 3OxoC12HSL-dependent, whereas ubiquitination at position 313 was not. ADP-ribosylation at position 124 appears to mediate another level of regulation that enhances asymmetry. In fact, the residue that is modified, D124, is the second residue of the dodecameric sequence

that is deleted in an inactive version of PON2 [49]. The results are important in light of the fact that such SNPs are involved in type 2 diabetes and its consequences.

**Supplementary Materials:** The following supporting information can be downloaded at: https://www.mdpi.com/article/10.3390/sym14020212/s1, Figure S1: SAXS-based reconstruction of the PON2 wild type structure.; Figure S2: Superposition of the wildtype and double mutant A148G_S311C.

**Author Contributions:** G.M. conceived the idea, wrote the paper and performed sequence and structure analysis; T.M.C. performed the experiments with FoldX, wrote and read the paper. All authors have read and agreed to the published version of the manuscript.

**Funding:** This research was funded by Ministry of University and Research (MUR), grant number POC01_00042.

**Institutional Review Board Statement:** Not applicable.

**Informed Consent Statement:** Not applicable.

**Data Availability Statement:** Data available from corresponding author.

**Conflicts of Interest:** The authors declare no conflict of interest.

## References

1. Goodsell, D.S.; Olson, A.J. Structural symmetry and protein function. *Annu. Rev. Biophys. Biomol. Struct.* **2000**, *29*, 105–153. [CrossRef]
2. Andrade, M.A.; Perez-Iratxeta, C.; Ponting, C.P. Protein repeats: Structures, functions, and evolution. *J. Struct. Biol.* **2001**, *134*, 117–131. [CrossRef]
3. Goodsell, D.S. Symmetry at the Cellular Mesoscale. *Symmetry* **2019**, *11*, 1170. [CrossRef]
4. Berchanski, A.; Segal, D.; Eisenstein, M. Modeling oligomers with Cn or Dn symmetry: Application to CAPRI target 10. *Proteins* **2005**, *60*, 202–206. [CrossRef]
5. Blundell, T.L.; Srinivasan, N. Symmetry, stability, and dynamics of multidomain and multicomponent protein systems. *Proc. Natl. Acad. Sci. USA* **1996**, *93*, 14243–14248. [CrossRef]
6. Mylemans, B.; Lee, X.Y.; Laier, I.; Helsen, C.; Voet, A.R.D. Structure and stability of the designer protein WRAP-T and its permutants. *Sci. Rep.* **2021**, *11*, 18867. [CrossRef]
7. Lucy, R. Forrest Structural Symmetry in Membrane Proteins. *Annu. Rev. Biophys.* **2015**, *44*, 311–337. [CrossRef]
8. Gross, M. Symmetry and complexity in protein oligomers. *Curr. Biol.* **2012**, *22*, R175–R177. [CrossRef]
9. Balaji, S. Internal symmetry in protein structures: Prevalence, functional relevance and evolution. *Curr. Opin. Struct. Biol.* **2015**, *32*, 156–166. [CrossRef]
10. Changeux, J.P. Allostery and the Monod–Wyman–Changeux model after 50 years. *Annu. Rev. Biophys.* **2012**, *41*, 103–133. [CrossRef]
11. André, I.; Strauss, C.E.M.; Kaplan, D.B.; Bradley, P.; Baker, D. Emergence of symmetry in homooligomeric biological assemblies. *Proc. Natl. Acad. Sci. USA* **2008**, *105*, 16148–16152. [CrossRef]
12. Kim, C.; Basner, J.; Lee, B. Detecting internally symmetric protein structures. *BMC Bioinform.* **2010**, *11*, 303. [CrossRef]
13. Myers-Turnbull, D.; Bliven, S.E.; Rose, P.W.; Aziz, Z.K.; Youkharibache, P.; Bourne, P.E.; Prlić, A. Systematic Detection of Internal Symmetry in Proteins Using CE-Symm. *J. Mol. Biol.* **2014**, *426*, 2255–2268. [CrossRef]
14. Beton, D.; Marana, S.R. Half-Barrels Derived from a (β/α)8 Barrel β-Glycosidase Undergo an Activation Process. *PLoS ONE* **2015**, *10*, e0139673. [CrossRef]
15. Liu, L.; Iwata, K.; Yohda, M.; Miki, K. Structural insight into gene duplication, gene fusion and domain swapping in the evolution of PLP-independent amino acid racemases. *FEBS Lett.* **2002**, *528*, 114–118. [CrossRef]
16. Kopec, K.O.; Lupas, A.N. β-Propeller blades as ancestral peptides in protein evolution. *PLoS ONE* **2013**, *8*, e77074, Erratum in *PLoS ONE* **2014**, *9*. [CrossRef]
17. Yadid, I.; Tawfik, D.S. Reconstruction of functional β-propeller lectins via homo-oligomeric assembly of shorter fragments. *Mol. Biol.* **2007**, *365*, 10–17. [CrossRef]
18. Chen, C.K.; Chan, N.L.; Wang, A.H. The many blades of the β-propeller proteins: Conserved but versatile. *Trends Biochem. Sci.* **2011**, *36*, 553–561. [CrossRef]
19. Harel, M.; Aharoni, A.; Gaidukov, L.; Brumshtein, B.; Khersonsky, O.; Meged, R.; Dvir, H.; Ravelli, R.B.G.; McCarthy, A.; Toker, L.; et al. Structure and evolution of the serum paraoxonase family of detoxifying and anti-atherosclerotic enzymes. *Nat. Struct. Mol. Biol.* **2004**, *11*, 412–419. [CrossRef]
20. Suruchi, A.; Banerjee Sanjay, K.; Chandra, T.N.; Kumar, Y.A. Post-translational Modification Crosstalk and Hotspots in Sirtuin Interactors Implicated in Cardiovascular Diseases. *Front. Genet.* **2020**, *11*, 356.

21. Wu, Z.; Huang, R.; Yuan, L. Crosstalk of intracellular post-translational modifications in cancer. *Arch. Biochem. Biophys.* **2019**, *676*, 108138. [CrossRef]
22. Lee, J.S.; Smith, E.; Shilatifard, A. The language of histone crosstalk. *Cell* **2010**, *142*, 682–685. [CrossRef]
23. Javaid, N.; Choi, S. Acetylation- and Methylation-Related Epigenetic Proteins in the Context of Their Targets. *Genes* **2017**, *8*, 196. [CrossRef]
24. Luo, M. Chemical and Biochemical Perspectives of Protein Lysine Methylation. *Chem. Rev.* **2018**, *118*, 6656–6705. [CrossRef]
25. Tak, I.; Ali, F.; Dar, J.S.; Magray, A.R.; Ganai, B.A.; Chishti, M.Z. Chapter 1—Posttranslational Modifications of Proteins and Their Role in Biological Processes and Associated Diseases. In *Protein Modificomics: From Modifications to Clinical Perspectives Tanveer Ali Dar*; Tanveer, A.D., Laishram, R.S., Protein, M., Eds.; Academic Press: Cambridge, MA, USA, 2019; pp. 1–35. ISBN 9780128119136.
26. Hyun, K.; Jeon, J.; Park, K.; Kim, J. Writing, erasing and reading histone lysine methylations. *Exp. Mol. Med.* **2017**, *49*, e324. [CrossRef]
27. Ramesh, V.; Krishnan, J. Symmetry breaking meets multisite modification. *eLife* **2021**, *10*, e65358. [CrossRef]
28. Khan, A.; McQuilken, M.; Gladfelter, A.S. Septins and Generation of Asymmetries in Fungal Cells. *Ann. Rev. Microbiol.* **2015**, *69*, 487–503. [CrossRef]
29. Wang, F. The signaling mechanisms underlying cell polarity and chemotaxis. *Cold Spring Harb. Perspect. Biol.* **2009**, *1*, a002980. [CrossRef]
30. Hargittai, I.; Hargittai, M. *Symmetry: A Unifying Concept*; Shelter Publications, Inc.: Bolinas, CA, USA, 1994.
31. Hochberg, D.; Bourdon García, R.D.; Ágreda Bastidas, J.A.; Ribó, J.M. Stoichiometric network analysis of spontaneous mirror symmetry breaking in chemical reactions. *Phys. Chem. Chem. Phys.* **2017**, *19*, 17618–17636. [CrossRef]
32. Ribó, J.M.; Hochberg, D.; Crusats, J.; El-Hachemi, Z.; Moyano, A. Spontaneous mirror symmetry breaking and origin of biological homochirality. *J. R. Soc. Interface* **2017**, *14*, 20170699. [CrossRef]
33. Hananel, U.; Ben-Moshe, A.; Diamant, H.; Markovich, G. Spontaneous and directed symmetry breaking in the formation of chiral nanocrystals. *Proc. Natl. Acad. Sci. USA* **2019**, *116*, 11159–11164. [CrossRef]
34. Kushida, Y.; Sawato, T.; Shigeno, M.; Saito, N.; Yamaguchi, M. Deterministic and Stochastic Chiral Symmetry Breaking Exhibited by Racemic Aminomethylenehelicene Oligomers. *Chem. Eur. J.* **2017**, *23*, 327–333. [CrossRef]
35. Soai, K.; Shibata, T.; Morioka, H.; Choji, K. Asymmetric autocatalysis and amplification of enantiomeric excess of a chiral molecule. *Nature* **1995**, *378*, 767–768. [CrossRef]
36. Chen, Y.; Ma, W. The origin of biological homochirality along with the origin of life. *PLoS Comput. Biol.* **2020**, *16*, e1007592. [CrossRef]
37. Blackmond, D.G. Autocatalytic Models for the Origin of Biological Homochirality. *Chem. Rev.* **2020**, *120*, 4831–4847. [CrossRef]
38. Ng, C.J.; Shih, D.M.; Hama, S.Y.; Villa, N.; Navab, M.; Reddy, S.T. The paraoxonase gene family and atherosclerosis. *Free Radic. Biol. Med.* **2005**, *38*, 153–163. [CrossRef]
39. Précourt, L.-P.; Amre, D.; Denis, M.-C.; Lavoie, J.-C.; Delvin, E.; Seidman, E.; Levy, E. The three-gene paraoxonase family: Physiologic roles, actions and regulation. *Atherosclerosis* **2011**, *214*, 20–36. [CrossRef]
40. Rothem, L.; Hartman, C.; Dahan, A.; Lachter, J.; Eliakim, R.; Shamir, R. Paraoxonases are associated with intestinal inflammatory diseases and intracellularly localized to the endoplasmic reticulum. *Free Radic. Biol. Med.* **2007**, *43*, 730–739. [CrossRef]
41. Horke, S.; Witte, I.; Wilgenbus, P.; Krüger, M.; Strand, D.; Förstermann, U. Paraoxonase-2 reduces oxidative stress in vascular cells and decreases endoplasmic reticulum stress-induced caspase activation. *Circulation* **2007**, *115*, 2055–2064. [CrossRef]
42. Hagmann, H.; Kuczkowski, A.; Ruehl, M.; Lamkemeyer, T.; Brodesser, S.; Horke, S.; Dryer, S.; Schermer, B.; Benzing, T.; Brinkkoetter, P.T. Breaking the chain at the membrane: Paraoxonase 2 counteracts lipid peroxidation at the plasma membrane. *FASEB J.* **2015**, *28*, 1769–1779. [CrossRef]
43. Draganov, D.I.; Teiber, J.F.; Speelman, A.; Osawa, Y.; Sunahara, R.; La Du, B.N. Human paraoxonases (PON1, PON2, and PON3) are lactonases with overlapping and distinct substrate specificities. *J. Lipid Res.* **2005**, *46*, 1239–1247. [CrossRef]
44. Teiber, J.F.; Horke, S.; Haines, D.C.; Chowdhary, P.K.; Xiao, J.; Kramer, G.L.; Haley, R.W.; Draganov, D.I. Dominant role of paraoxonases in inactivation of the Pseudomonas aeruginosa quorum-sensing signal N-(3-oxododecanoyl)-l-homo-serine lactone. *Infect. Immun.* **2008**, *76*, 2512–2519. [CrossRef]
45. Schuster, M.; Sexton, D.J.; Diggle, S.P.; Greenberg, E.P. Acyl-homoserine lactone quorum sensing: From evolution to application. *Annu. Rev. Microbiol.* **2013**, *67*, 43–63. [CrossRef]
46. Liu, Y.C.; Chan, K.G.; Chang, C.Y. Modulation of host biology by Pseudomonas aeruginosa quorum sensing signal molecules: Messengers or traitors. *Front. Microbiol.* **2015**, *6*, 1226. [CrossRef]
47. Manco, G.; Porzio, E.; Carusone, T.M. Human Paraoxonase-2 (PON2): Protein Functions and Modulation. *Antioxidants* **2021**, *10*, 256. [CrossRef]
48. Mandrich, L.; Cerreta, M.; Manco, G. An Engineered Version of Human PON2 Opens the Way to Understand the Role of Its Post-Translational Modifications in Modulating Catalytic Activity. *PLoS ONE* **2015**, *10*, e0144579. [CrossRef]
49. Carusone, T.M.; Cardiero, G.; Cerreta, M.; Mandrich, L.; Moran, O.; Porzio, E.; Catara, G.; Lacerra, G.; Manco, G. WTAP and BIRC3 are involved in the posttranscriptional mechanisms that impact on the expression and activity of the human lactonase PON2. *Cell Death Dis.* **2020**, *324*, 1–17. [CrossRef]
50. Jumper, J.; Evans, R.; Pritzel, A.; Green, T.; Figurnov, M.; Ronneberger, O.; Tunyasuvunakool, K.; Bates, R.; Žídek, A.; Potapenko, A.; et al. Highly accurate protein structure prediction with AlphaFold. *Nature* **2021**, *596*, 583–589. [CrossRef]

51. Guex, N.; Peitsch, M.C.; Schwede, T. Automated comparative protein structure modeling with SWISS-MODEL and Swiss-PdbViewer: A historical perspective. *Electrophoresis* **2009**, *30*, S162–S173. [CrossRef]
52. Schymkowitz, J.; Borg, J.; Stricher, F.; Nys, R.; Rousseau, F.; Serrano, L. The FoldX web server: An online force field. *Nucleic Acids Res.* **2005**, *33*, W382–W388. [CrossRef]
53. Available online: https://evosite3d.blogspot.com/2015/03/tutorial-estimating-stability-effect-of.html (accessed on 11 November 2021).
54. Krieger, E.; Vriend, G. YASARA View—Molecular graphics for all devices—From smartphones to workstations. *Bioinformatics* **2014**, *30*, 2981–2982. [CrossRef]
55. Jumper, J.; Evans, R.; Pritzel, A.; Green, T.; Figurnov, M.; Ronneberger, O.; Tunyasuvunakool, K.; Bates, R.; Žídek, A.; Potapenko, A.; et al. Highly accurate protein structure prediction for the human proteome. *Nature* **2021**, *596*, 590–596. [CrossRef]
56. Akimov, V.; Barrio-Hernandez, I.; Hansen, S.V.F.; Hallenborg, P.; Pedersen, A.K.; Bekker-Jensen, D.B.; Puglia, M.; Christensen, S.D.K.; Vanselow, J.T.; Nielsen, M.M.; et al. UbiSite approach for comprehensive mapping of lysine and N-terminal ubiquitination sites. *Nat. Struct. Mol. Biol.* **2018**, *25*, 631–640. [CrossRef]
57. Primo-Parmo, S.L.; Sorenson, R.C.; Teiber, J.; Du, B.N. The Human Serum Paraoxonase/Arylesterase Gene (PON1) Is One Member of a Multigene Family. *Genomics* **1996**, *33*, 498–507. [CrossRef] [PubMed]
58. Aviram, M.; Billecke, S.; Sorenson, R.; Bisgaier, C.; Newton, R.; Rosenblat, M.; Erogul, J.; Hsu, C.; Dunlop, C.; La Du, B. Paraoxonase Active Site Required for Protection Against LDL Oxidation Involves Its Free Sulfhydryl Group and Is Different from That Required for Its Arylesterase/Paraoxonase Activities. *Arter. Thromb. Vasc. Biol.* **1998**, *18*, 1617–1624. [CrossRef]